A SUBSPACE-BASED CHANNEL MODEL FOR FREQUENCY SELECTIVE TIME VARIANT MIMO CHANNELS

Giovanni Del Galdo, Martin Haardt, and Marko Milojević
Ilmenau University of Technology - Communications Research Laboratory
PO Box 100565, 98684 Ilmenau, Germany
{giovanni.delgaldo, martin.haardt}@tu-ilmenau.de

Abstract - In this contribution we propose a subspace-based channel model suitable to represent frequency selective time variant MIMO channels. This approach captures the true nature of the MIMO channel maintaining the spatial correlation present between the antenna arrays. Correlation in time and frequency is conserved as well. The decomposition into eigenmodes, which form the channel subspace, gives an interesting interpretation of the channel's eigenstructure. These investigations lead to a very efficient method to synthesize new channels with the same correlation in time, frequency and space of a reference channel. The model allows the interpolation of a channel in order to retrieve more samples in frequency and time to perform statistical analysis such as bit error rate and capacity curves. In addition the model allows the generation of new random channels with the same spatial, time, and frequency correlations of a reference channel.

Keywords - MIMO, modelling, subspace

I. INTRODUCTION

A time variant frequency selective SISO channel can be conveniently stored in form of a matrix in one of the four two-dimensional Bello domains [1]. Either $\{t, f\}$, $\{t, \tau\}$, $\{f_{\mathrm{D}}, f\}$ or $\{f_{\mathrm{D}}, \tau\}$ where t, f_{D}, f, and τ denote time, Doppler frequency, frequency, and delay time, respectively. When dealing with MIMO systems we need one of these SISO matrices for each pair of antennas. If we choose $\{t, f\}$, the channel matrix becomes a four-dimensional array $\boldsymbol{H} \in \mathbb{C}^{M_R \times M_T \times N_f \times N_t}$, where M_R and M_T are the number of antennas at the receiver and at the transmitter, whereas N_f and N_t are the number of samples taken in frequency and time, respectively. Such a data structure requires a large amount of parameters to store, namely $M_{\mathrm{R}} \cdot M_{\mathrm{T}} \cdot N_f \cdot N_t$. This subspace-based model allows us to drastically reduce the number of parameters needed to describe the channel.

Section II illustrates the data model and the proposed channel model. Section III deals with the interpolation of the channel. Finally, section IV draws the conclusions.

The proposed processing algorithms can be extended to other applications such as channel estimation for multi-carrier systems, transmit beamforming schemes, and the generation of uncorrelated realizations of the same channel for statistical analysis.

II. THE SUBSPACE-BASED MODEL

The channel for a specific frequency bin f_0 and time snapshot t_0 appears as a two-dimensional matrix $\boldsymbol{H}_{f_0,t_0}$ of size $M_R \times M_T$. Applying the $\mathrm{vec}\{\cdot\}$ operator to this matrix gives a vector $\boldsymbol{h}_{f_0,t_0}$ so that

$$\boldsymbol{h}_{f_0,t_0} = \mathrm{vec}\{\boldsymbol{H}_{\mathrm{f}_0,\mathrm{t}_0}\} \in \mathbb{C}^{M_{\mathrm{R}} \cdot M_{\mathrm{T}} \times 1} \tag{1}$$

The joint spatial correlation matrix $\boldsymbol{R}_{\mathrm{H}}$ for f_0 and t_0 can be written as:

$$\boldsymbol{R}_{\mathrm{H}}(f_0, t_0) = \mathrm{E}\{\boldsymbol{h}_{f_0,t_0} \cdot \boldsymbol{h}_{f_0,t_0}^{\mathrm{H}}\} \in \mathbb{C}^{M_R \cdot M_T \times M_R \cdot M_T} \tag{2}$$

where the superscript $^{\mathrm{H}}$ denotes the hermitian transpose.

We extend the flat fading channel representation proposed in [2] to a frequency selective time variant channel, exploiting the correlation in the frequency and time domain. This model takes advantage of the spatial correlation of the channel, considering its eigenstructure.

From the joint spatial correlation matrix we can obtain the unitary matrix $\boldsymbol{U}$ of dimensions $M_R \cdot M_T \times M_R \cdot M_T$ via the eigenvalue decomposition:

$$\boldsymbol{R}_{\mathrm{H}}(f_0, t_0) = \boldsymbol{U} \cdot \boldsymbol{\Lambda} \cdot \boldsymbol{U}^{\mathrm{H}}. \tag{3}$$

The matrix $\boldsymbol{U}$ contains the eigenvectors of $\boldsymbol{R}_{\mathrm{H}}(f_0, t_0)$ and represents a full basis for the space in which $\boldsymbol{h}_{f_0,t_0}$ is defined. In other words, it is possible to write $\boldsymbol{h}_{f_0,t_0}$ as a linear combination of the column vectors present in $\boldsymbol{U}$, as

$$\boldsymbol{h}_{f_0,t_0} = \sum_{k=1}^{M_{\mathrm{R}} M_{\mathrm{T}}} \gamma_{f_0,t_0}^{(k)} \cdot \boldsymbol{u}^{(k)} \tag{4}$$

where $\boldsymbol{u}^{(k)}$ is the k-th eigenvector.

The factor $\gamma_{f_0,t_0}^{(k)}$ can be calculated as the projection of the vector $\boldsymbol{h}$ onto the k-th vector of the basis:

$$\gamma_{f_0,t_0}^{(k)} = (\boldsymbol{u}^{(k)})^{\mathrm{H}} \cdot \boldsymbol{h}_{f_0,t_0}. \tag{5}$$

Note that if $\boldsymbol{h}_{f_0,t_0} = \mathrm{E}\{\boldsymbol{h}_{f_0,t_0}\}$, then $\gamma_{f_0,t_0}^{(k)} = \lambda^{(k)}$ where $\lambda^{(k)}$ is the k-th eigenvalue, i.e., the k-th element on the diagonal of $\boldsymbol{\Lambda}$.

We can decompose the channel for a different frequency f_1 and time t_1 in a similar way, using the same basis $\boldsymbol{U}$ while applying different weights:

$$\boldsymbol{h}_{f_1,t_1} = \sum_{k=1}^{M_{\mathrm{R}} M_{\mathrm{T}}} \gamma_{f_1,t_1}^{(k)} \cdot \boldsymbol{u}^{(k)}. \tag{6}$$

It is possible to parametrize the channel at different frequencies and times, using a common low-rank basis, by means of storing the different γ's for each specific time and frequency bin.

In fact, in most channels the number of significant weights is much smaller than their total number. Therefore we can introduce a low-rank approximation using only the first L strongest basis vectors, i.e., the ones which correspond to the strongest weights, forming a new reduced basis $\tilde{\boldsymbol{U}}$ of size $M_R \cdot M_T \times L$.

$$\tilde{\boldsymbol{h}}_{f_0,t_0} = \sum_{k=1}^{L} \gamma^{(k)}_{f_0,t_0} \cdot \tilde{\boldsymbol{u}}^{(k)}. \tag{7}$$

Clearly, with a full basis it is always possible to decompose an arbitrary complex vector $\boldsymbol{h}_{f,t}$ as in eq. (6). However in order to decompose it with good precision with a reduced basis, it is necessary for $\boldsymbol{h}_{f,t}$ to lie in the subspace spanned by the columns of $\tilde{\boldsymbol{U}}$. This occurs in practice if $\boldsymbol{h}_{f,t}$ is chosen in the vicinity of f_0 and t_0, namely within the coherence bandwidth and coherence time.

In order to parametrize a channel we have to calculate from the available data an estimate $\hat{\boldsymbol{R}}_{\mathrm{H}}$ for the joint spatial correlation matrix $\boldsymbol{R}_{\mathrm{H}}$.

$$\hat{\boldsymbol{R}}_{\mathrm{H}} = \sum_{t \in T} \sum_{f \in F} \boldsymbol{h}_{f,t} \cdot \boldsymbol{h}^{\mathrm{H}}_{f,t}, \tag{8}$$

where T and F represent the domains in time and frequency in which the averaging is performed.

From $\hat{\boldsymbol{R}}_{\mathrm{H}}$ we calculate $\boldsymbol{U}$ and consequently the reduced basis $\tilde{\boldsymbol{U}}$ which is used to decompose all bins within T and F.

If the averaging window in time and frequency is small enough, a reduced basis made up of very few eigenvectors will be sufficient to accurately reconstruct the channel matrices. In our simulations we have confirmed that the maximum size of the averaging windows to keep a small error while having the smallest number of basis vectors is comparable to the coherence time and coherence bandwidth.

If we average over a larger window we can still apply a low-rank approximation but we would need more vectors to keep the error small.

Within a small window the channel possesses the same spatial subspace. This means that the joint spatial correlation matrix of every point in the window is the same and thus will be mapped by the same eigenbasis. If the channel is not totally uncorrelated, i.e., there exist some dominant paths, only a part of the eigenvalues of $\hat{\boldsymbol{R}}_{\mathrm{H}}$ will be significant. This leads to the possibility of deriving a low-rank approximation.

As we sum more frequencies outside the coherence bandwidth, $\hat{\boldsymbol{R}}_{\mathrm{H}}$ becomes richer, meaning that more eigenvalues become significant. However, the number of vectors needed for the low-rank approximation grows very slowly with frequency because the subspaces which are summed are partially overlapping. This means in practice that one or two vectors added to the basis are enough to cover a frequency window 3 to 4 times longer than the coherence bandwidth. The subspaces corresponding to different frequencies overlap because they depend strictly on the Directions of Arrival (DoA) and on the Directions of Departure (DoD), which are of course the same for every frequency. However, the overlap is not perfect, because the antenna arrays see the DoA and DoD differently for different frequencies. For instance, the response of the m-th sensor in a Uniform Linear Array (ULA) for an impinging wave coming from an angle θ is $\mathrm{e}^{-j \cdot \frac{2\pi}{\lambda} \Delta (m-1) \cdot \sin(\theta)}$, where Δ is the spacing between the antennas and λ is the wavelength. This frequency dependency partially moves the subspace obliging us to take more vectors to describe the channel accurately at all frequencies. A quantitative and more detailed investigation on the decomposition error can be found in [3].

A. The Eigenmodes - A Physical Interpretation

The decomposition seen in eq. (3) can be rewritten so that the vector $\boldsymbol{u}^{(k)}$ is reshaped column-wise into the matrix:

$$\boldsymbol{\Theta}^{(k)} = \mathrm{unvec}\{\boldsymbol{u}^{(\mathrm{k})}\} \in \mathbb{C}^{M_{\mathrm{R}} \times M_{\mathrm{T}}}, \tag{9}$$

which we will refer to as the k-th *eigenmode*. Equation (3) becomes:

$$\boldsymbol{H}_{f_0,t_0} = \sum_{k=1}^{M_{\mathrm{R}} M_{\mathrm{T}}} \gamma^{(k)}_{f_0,t_0} \cdot \boldsymbol{\Theta}^{(k)}. \tag{10}$$

If the antenna arrays are ULAs at both ends, it is possible to reveal the physical interpretation of the matrix $\boldsymbol{\Theta}^{(k)}$. Through a two-dimensional Fourier transform the eigenmode can be directly transformed into the corresponding azimuthal spectrum. In this domain the Directions of Departure (DoD) and Directions of Arrival (DoA) are expressed in the $\mu_{\mathrm{R}}, \mu_{\mathrm{T}}$ domain, i.e., the spatial frequencies. The following equation permits us to translate them into the physical angles θ_{R} and θ_{T}:

$$\mu = -\frac{2\pi}{\lambda} \cdot \sin(\theta) \cdot \Delta. \tag{11}$$

Figures 1 and 2 show the azimuthal spectra of the first two $\boldsymbol{\Theta}s$ derived from a flat-fading, static channel in which only two paths exist. The channel was generated with the IlmProp [4]. The antenna arrays at the receiver and at the transmitter are ULAs consisting of 8 elements each. In this case the first two eigenmodes have rank one and each one represents a specific path. For richer channels, i.e., with more paths, the significant eigenmodes can reach higher ranks. This simply means that more than one path is represented by the same eigenmode.

This geometrical interpretation suggests that the subspaces should not change rapidly in time and frequency in the channels in which the DoD and DoA vary slowly. In case of other antenna geometries it is more complicated to derive the azimuthal spectra. It is however true that the eigenmodes reflect the physical paths, as explained in [3].

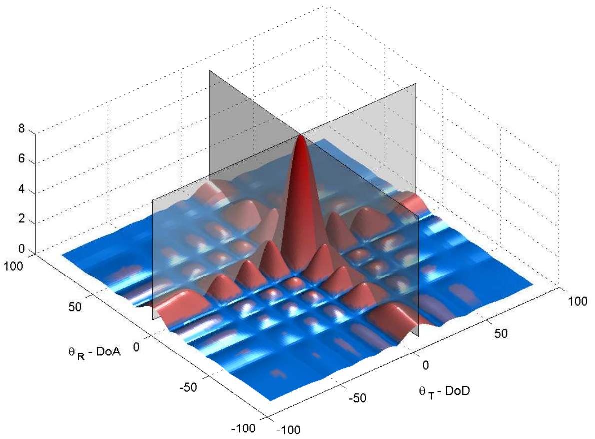

Fig. 1
Amplitude of the Azimuthal Spectrum of the strongest eigenmode. This matrix represents the path for $\theta_{\mathrm{R}} = 10°$ and $\theta_{\mathrm{T}} = 10°$.

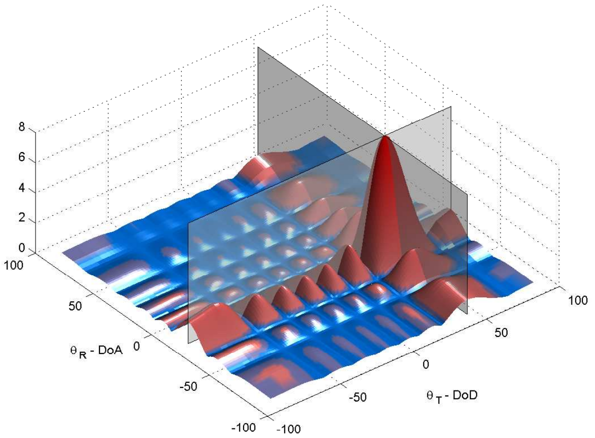

Fig. 2
Amplitude of the Azimuthal Spectrum of the second strongest. This matrix represents the path for $\theta_{\mathrm{R}} = -30°$ and $\theta_{\mathrm{T}} = 45°$.

B. *Correlation in Frequency and Time*

Figure 3 shows a synthetic model generated with the IlmProp in which an object has been properly set in order to obscure the Line Of Sight component during the second half of the simulation time. The transmitter (Tx) moves at a constant speed of 30 km/h. Both ends have a Uniform Linear Array (ULA) of five omnidirectional antennas each, parallel to the trajectory. The spacing between the antennas is $\frac{\lambda_0}{2}$, where λ_0 is the wavelength corresponding to the center frequency $f_0 = 2$ GHz. The sampling is characterized by sampling periods of $\Delta t = 3$ ms and $\Delta f = 600$ kHz

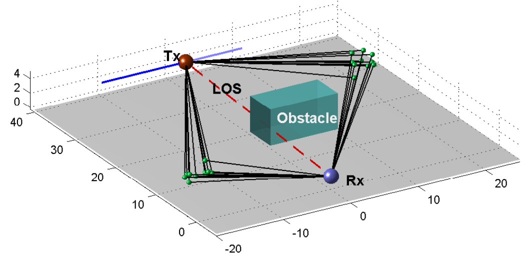

Fig. 3
Model generated with the IlmProp. The Line of Sight (LOS) is obstructed by an obstacle for half of the experiment time. The transmitter (Tx) moves linearly on the blue trajectory. The green balls represent scatterers which are always visible.

in the time and frequency domain, respectively. The total experiment time is 2.5 seconds and the bandwidth is 120 MHz. The channel is well sampled in both domains, meaning that no aliasing affects the results. The Rician K-factor [5], defined as power of the Line Of Sight (LOS) component divided by the total power of the scatterers, is approximately 10 when the terminals see each other, and obviously 0 otherwise. A white complex Gaussian noise floor is added so that the average SNR is 20 dB. The frequency selectiveness is guaranteed by two scatterering cluster which introduce multipath. One of the two clusters, as a whole, generates a path which is 3 dB stronger. The coherence bandwidth $(\Delta f)_{\mathrm{c}}$ calculated as in [5] is approximately 80 MHz. The decomposition seen in equation (7) is applied to the channel generated with this model. The matrix $\hat{\boldsymbol{R}}_{\mathrm{H}}$ is calculated as in equation (8) over all frequencies for each time snapshot. Figure 4 shows the amplitude of the first two γ's expressed in dB. In the first half (until approximately 1 second) the transmitter has clear LOS. The first eigenmode maps the direct link while the second and the third eigenmodes map the other two directions. The power of the LOS is very stable and it is affected only marginally by fast-fading. In fact the multipath components have overall 10 dB less power. As a result $\gamma^{(1)}$ is also very stable. The second eigenmode is however much more variable in strength since the echoes are characterized by substantial fluctuations being the sum of several rays, each one with a different phase due to the slightly different length. When moving into the NLOS part the line of sight component abruptly disappears. The first eigenmode now on maps the strongest echo. In Figure 4 it can be observed that at some times and frequencies the second eigenmode has more energy than the first. This happens due to the strong fading in time and frequency which affects the echoes. When the echo mapped by the first eigenmode experiences a fade, then the second echo might be stronger and $\gamma^{(2)}$ will thus be bigger than $\gamma^{(1)}$. When analyzing

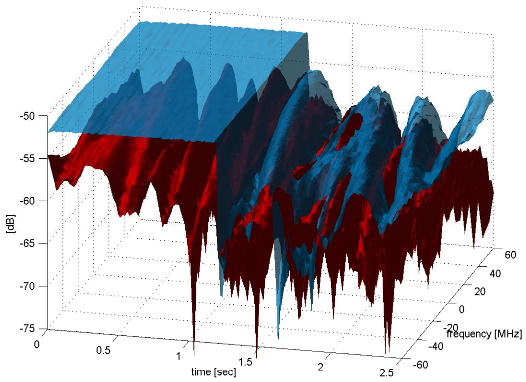

Fig. 4
Amplitude of the two strongest weights against time and frequency for an IlmProp channel.

the weights corresponding to higher order eigenmodes, we notice that they appear increasingly uncorrelated in time and frequency. This occurs because their eigenmodes map only the noise. The amplitudes of their weights are in fact Rayleigh distributed.

In order to validate the model on realistic channels we analyzed several MIMO measurements gathered at Ilmenau University of Technology with a RUSK channel sounder [6]. In all measurements we observed the same degree of correlation in the weights as seen with synthetic data.

When the eigenmode $\boldsymbol{\Theta}^{(k)}$ maps one path only, i.e., it has rank 1, it is interesting to note that the trend of the phase of the corresponding weight $\lambda^{(k)}$ decreases linearly with frequency. This phenomenon can be clearly observed in Figure 5, which shows the phase of the strongest weight, $\gamma^{(1)}$ for a measured channel. The linear phase is due to the

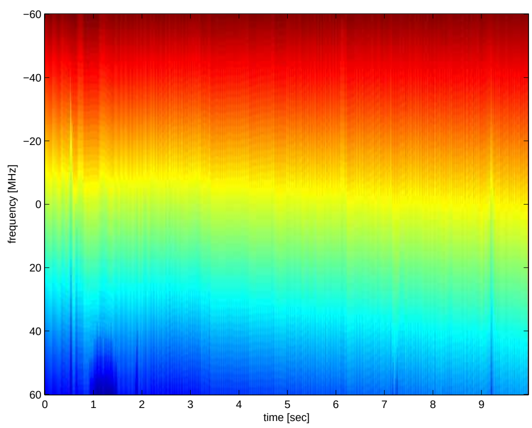

Fig. 5
Unwrapped phase of the strongest weight plotted against time and frequency for a measured channel.

propagation delay of the path. For a given time t_0, let τ_0 be the propagation delay, i.e., the length of the path divided by the speed of light. Then the phase $\varphi(t_0, f)$ will have the following expression:

$$\varphi(t_0, f) = e^{-j2\pi\tau_0 f}. \quad (12)$$

III. Interpolating the Channel

The subspace-based channel model proposed in this paper allows us to efficiently interpolate a channel in order to retrieve more samples to perform statistical analyses. Each weight γ can be separately interpolated to obtain a much denser sampling grid in time and frequency. The reconstruction at a specific time and frequency takes place using the interpolated weights and the basis which was calculated in the corresponding window. This technique can be successfully applied on channel measurements because it suppresses the noise present in the channel. In order to validate this method we compare the interpolation done via the subspace-based model and the trivial interpolation of the channel array, i.e., interpolating the channel matrix for each antenna pair.

Let $\boldsymbol{H}_{\rm full}$ be the sum of $\boldsymbol{H}_{\rm calc}$, the channel matrix with the signal component only, and $\boldsymbol{H}_{\rm n}$, the noise matrix. From the downsampling in frequency and time of $\boldsymbol{H}_{\rm full}$ we obtain $\boldsymbol{H}_{\rm down}$ which is then interpolated back to the original size with the two methods. Let $\boldsymbol{H}_{\rm ssb}$ be the channel array obtained via the subspace-based model and $\boldsymbol{H}_{\rm inter}$ the one obtained with a straightforward interpolation. Note that both interpolations are calculated from the noisy downsampled version of the channel, $\boldsymbol{H}_{\rm down}$. The channel matrix $\boldsymbol{H}_{\rm ssb}$ has been reconstructed as in equation (7) with $L = 3$.

Figure 6 shows the Cumulative Distribution Functions (CDF) of the capacity of a frequency selective channel generated with the IlmProp. The CDFs are calculated as in [5] for an SNR of 10 dB. The channel is characterized by a bandwidth of 5 MHz and 21 frequency bins. The downsampling factor is 2. For the left plot we assume no Channel State Information (CSI) while for the right one the waterfilling algorithm has been applied in a case of perfect channel knowledge. The CDF obtained from $\boldsymbol{H}_{\rm calc}$ reflects the true capacity of the channel. The CDF of $\boldsymbol{H}_{\rm inter}$ approaches the one of $\boldsymbol{H}_{\rm full}$ because in the interpolation process the noise has not been removed. On the other hand, the curve resulting from $\boldsymbol{H}_{\rm ssb}$ successfully approaches $\boldsymbol{H}_{\rm calc}$ having reconstructed the signal subspace only.

Another application for the subspace-based channel model proposed is the *synthesis* of new random channels with the same spatial, time, and frequency correlations of a reference channel. From a reference channel $\boldsymbol{H}_{\rm ref}$ we can calculate the complete set of eigenmodes $\boldsymbol{\Theta}_{\rm ref}$ and of weights $\gamma_{\rm ref}$ as previously described in section II. Using equation (10) read from right to left, we can synthesize a new channel applying the same eigenmodes $\boldsymbol{\Theta}_{\rm ref}$, while generating new random

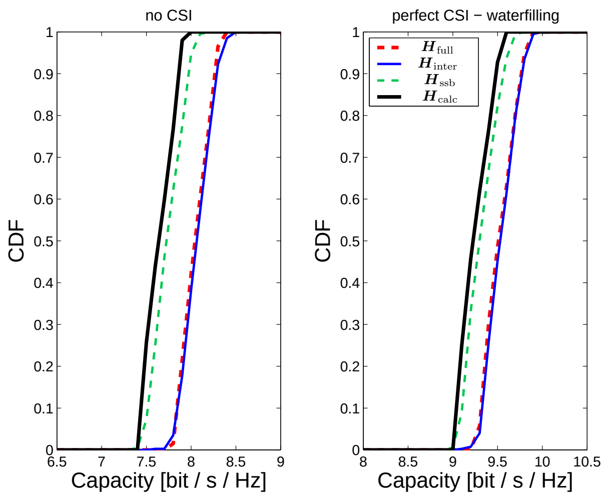

Fig. 6

Cumulative Distribution Functions (CDF) of the capacity of a frequency selective channel generated with the IlmProp. The curve for $\boldsymbol{H}_{\rm full}$ and $\boldsymbol{H}_{\rm calc}$ correspond to the noisy and noiseless channel, respectively. The curves for $\boldsymbol{H}_{\rm inter}$ and $\boldsymbol{H}_{\rm calc}$ are for the interpolated channels.

γ's. Preserving the same eigenmodes assures that the new channel will have the same correlation in space. In order to achieve the same correlation in frequency and time the new γ's must be generated very carefully. The k-th weight $\gamma_{\rm ref}^{(k)}$ can be seen as a realization of a two-dimensional stochastic process in time and frequency whose Power Spectral Density (PSD) can be estimated via one of the numerous techniques available in the literature. The process can be assumed wide sense stationary across frequency and time variant across time. Once the PSD is known it is possible to generate a new set of γ's via a 2D inverse Fourier transform of $\Gamma^{(k)}(f_{\rm D}, \tau)$. The function $\Gamma^{(k)}(f_{\rm D}, \tau)$ is calculated so that its absolute value is the square root of the PSD, while its phase is a random number uniformly distributed in $[0, 2\pi]$ for every $f_{\rm D}$ and τ. The realizations generated in such a way can be processed for any kind of statistical analysis, such as capacity and bit error rate curves. The results characterize a channel with the same characteristics in space, time, and frequency.

IV. Conclusions

In this paper we propose a channel parametrization which models frequency selective time variant MIMO channels. In particular we emphasize how the channel's correlation in space, time, and frequency is accurately reproduced in the model. The subspaces in which the channel is decomposed, possess a strong physical interpretation which is illustrated thanks to the synthetic channels generated with the IlmProp. The model allows the interpolation of a channel in order to retrieve more samples in frequency and time to perform statistical analysis such as bit error rate and capacity curves. In addition the model allows the generation of new random channels with the same correlation in space, time, and frequency of a reference channel.

Acknowledgements

The authors gratefully acknowledge the support of MEDAV (www.channelsounder.de) in performing the channel measurements.

This work was partly sponsored by the European Network of Excellence NEWCOM.

References

[1] P. Bello, "Characterization of randomly time-variant linear channels," *IEEE Trans. Comm. Syst.*, vol. 11, pp. 360–393, 1963.

[2] E. Bonek, W. Weichselberger, A.F. Molisch, and H. Hofstetter, "MIMO channel model revisited," COST Workshop Tutorial, Prague, Sept. 2003.

[3] G. Del Galdo, M. Milojevic, M. Haardt, and M. Hennhöfer, "Efficient channel modelling for frequency selective MIMO channels," *in Proc. ITG Workshop on Smart Antennas, Munich*, Mar. 2004.

[4] G. Del Galdo, J. Lotze, M. Haardt, and C. Schneider, "Advanced geometry-based modeling for MIMO scenarios in comparison with real measurements," in *Proc. 48. Internationales Wissenschaftliches Kolloquium*, Ilmenau, Germany, Sept. 2003.

[5] R. Nabar A. Paulraj and D. Gore, *Introduction to space-time wireless communications*, Cambridge University Press, Cambridge, 2003.

[6] R.S. Thomä, D. Hampicke, A. Richter, G. Sommerkorn, and U. Trautwein, "MIMO vector channel sounder measurement for smart antenna system evaluation," *European Transaction on Telecommunications, Special issue on smart antennas*, vol. 12, no. 5, 2001.